Science through Scanning Probe Microscopy 2016 (StSPM'16)

20 – 21 ottobre 2016, Bologna, CNR – Area della Ricerca

Il workshop Science through Scanning Probe Microscopy 2016 (StSPM'16), organizzato dall'Istituto per lo Studio dei Materiali Nanostrutturati (ISMN) e dalla Società Italiana di Scienze Microscopiche (SISM), in collaborazione con l'Area della Ricerca di Bologna, ha replicato il successo dell'edizione 2013 raccogliendo circa 60 ricercatori provenienti da molte regioni italiane, dal sud fino al nord, afferenti ad università, enti di ricerca e laboratori industriali, ma soprattutto ha visto la partecipazione di molti giovani ricercatori.

StSPM'16 ha mostrato una comunità SPM viva, in linea con i più recenti avanzamenti scientifici nelle due macro-aree principali della scienza dei materiali e della vita. Una menzione speciale va a Bruno Samorì, il quale, con eleganza e sobrietà, ha aperto i lavori del workshop raccontando un frammento della storia della microscopia attraverso la sua carriera. Sono stati presentati 29 contributi orali, di cui 9 ad invito per professori e ricercatori di chiara fama. I contributi delle due macro-aree sono stati alternati per mantenere costante l'attenzione dei partecipanti e condensati nel pomeriggio del 20 e nella mattina del 21 Ottobre. L'ambiente collaborativo e spontaneo che si è instaurato ha permesso a tutti i partecipanti, studenti inclusi, di sentirsi liberi di fare domande, proporre idee e discutere.

Di fondamentale importanza alla riuscita dell'evento è stata la partecipazione e il contributo economico delle ditte SPM, sponsor dell'evento e della SISM. In tutto hanno partecipato 11 rappresentanti di 10 ditte connesse alla microscopia a scansione di sonda. La loro partecipazione è stata valorizzata da una sessione speciale dove sono state presentate le ultime novità commerciali in quanto a microscopi, sonde ed accessori. La sessione è stata organizzata in stile "Elevator pitch", ovvero l'oratore doveva descrivere la propria ditta sinteticamente, chiaramente ed efficacemente nei limiti di tempo imposti dalla corsa dell'ascensore (specificatamente 10 minuti). Il risultato è stata una sessione frizzante e snella da seguire.

Infine, seguendo lo spirito educativo della SISM, abbiamo colto l'occasione del workshop per realizzare questi proceeding su "Microscopie", la rivista della società. Al momento, la rivista è indicizzata DOI, ma speriamo di assegnarle un Impact Factor internazionale nel prossimo futuro.

Ringraziamo pubblicamente tutti coloro che hanno partecipato all'organizzazione e hanno supportato l'iniziativa in qualsiasi forma e, per concludere, vi aspettiamo a StSPM'19 dove, siamo convinti, parteciperete con entusiamo e nuovi risutalti scientifici.

Il comitato scientifico

Cristiano Albonetti
Francesco Valle
Marco Brucale

Magnetic force microscopy with controlled magnetization of the tip: Toward truly quantitative nanomagnetometry

L. Angeloni,[1,2] D. Passeri,[1] M. Natali,[1] M. Reggente,[1,3] D. Mantovani,[2] M. Rossi[1,4]

[1]*Department of Basic and Applied Sciences for Engineering; University of Rome Sapienza; Via A. Scarpa 14, 00161 Rome, Italy*
[2]*Department Min-Met-Materials Eng. & University Hospital Research Center; Laval University; Quebec City, Canada*
[3]*Institut de Physique et Chimie des Matériaux de Strasbourg (IPCMS), UMR 7504 CNRS-Université de Strasbourg, 23 rue du Loess, BP 43 67034, Strasbourg – France*
[4]*Research Center for Nanotechnology applied to Engineering of SAPIENZA University of Rome (CNIS), Piazzale A. Moro 5, 00185 Rome, Italy*

Corresponding author: Dr. D. Passeri (daniele.passeri@uniroma1.it)

Key words: nanoparticles, Magnetic Force Microscopy, Atomic Force microscopy

Introduction

Magnetic nanoparticles exhibit very particular magnetic properties (superparamagnetic character), which can be exploited in several diagnostic and therapeutic applications.[1] The development and optimization of these systems require a deep understanding of the magnetic behavior of the used nanomaterials, and, therefore, a detailed characterization of their main magnetic properties. NPs systems are conventionally characterized by statistical techniques which allow the measurement of the overall magnetic parameters of numerous ensembles of NPs in the form of patterns or ferrofluids, which, however, do not allow the complete comprehension of all the mechanisms regulating the magnetic NPs system behavior, such as the dependence with other chemical and physical properties (e.g. the composition, the structure, the size, the shape) and the effects of the mutual inter-particles dipolar interactions. For this reason several efforts are focused on the development of high resolution and nano-element sensitive techniques able to measure the magnetic parameters of single nanoparticles and, thus, deepen the understanding of all the factors influencing the magnetic behavior of single elements and affecting the efficiency of the overall system. Among other high resolution techniques, Magnetic Force Microscopy, thanks to its nanometric lateral resolution, high sensitivity, applicability to all kind of magnetic nanomaterials without particular sample preparation and not expensive instrumental apparatus, is emerging as a potential tool for the characterization of single magnetic nanomaterials.

Nevertheless, some open issues have been identified as the main drawbacks limiting the application of the technique to the quantitative magnetic characterization of single magnetic nanoparticles, which can be summarize as follows: i) the presence of non-magnetic tip-sample interactions, which produce an additional signal in MFM measurements, making difficult the extrapolation of the "pure" magnetic contribution and, therefore, the quantitative interpretation of the measured data; ii) the lack of a theoretical model describing the magnetic tip-NPs interactions consistently with experimental data and the consequent difficulty in "converting" the measured data in the values of real physical parameters such as the NP magnetization.[2]

The evidence of the necessity of a methodology to evaluate and eliminate the electrostatic effects in MFM images encouraged us to conceive a new MFM approach, we called Controlled Magnetization MFM (CM-MFM), with the aim of depurating MFM images from electrostatic contributions and detect the pure magnetic signal.

In this work we present a synthesis of the results obtained with CM-MFM technique and its possible applications.

Materials and Methods

In CM-MFM, two subsequent MFM images of the same area are collected. Each MFM image is acquired using the so called "lift height mode". The first MFM image, an example of which is reported in Figure 1 a), is acquired using the probe magnetized along a certain direction, allowing the measurement of the signal resulting by the superimposition of the electrostatic and the magnetic tip-sample interactions. Then, a second image is detected using the probe "demagnetized", allowing the detection of the contribution due to the sole electrostatic effects, as shown in the example reported in Figure 1 b). The image representative of the "pure" magnetic signal is retrieved by subtracting the second image to the first one. An example is reported in Figure 1 c). The in situ demagnetization of the probe (i.e. without moving the probe from the scan area) is obtained through the application of its remanent coercitive magnetic field, determined by a calibration procedure performed using a reference sample with periodically patterned magnetic domains and measuring

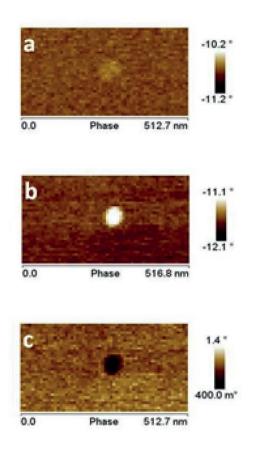the phase contrast in two adjacent domains after applying and switching off magnetic fields with different intensity.[3]

Figure 1. Standard MFM image (a), electrostatic image (b) and CM-MFM image (c) obtained by the subtraction of image (b) to image (a) of a Fe$_3$O$_4$ NP of 18nm (diameter).

Results and Conclusions

The effectiveness of CM-MFM technique has been demonstrated through a challenging case study, i.e., the characterization of superparamagnetic NPs in absence of any applied external magnetic field.[3] Once the electrostatic artifacts are removed, the tip-NP interaction has been demonstrated to be well described by that of two single-point magnetic dipoles, indicating the effectiveness of our technique in the removal of electrostatic artifacts in MFM maps and the possibility of retrieving quantitative information about single NPs properties.

As an example, a possible application of CM-MFM consists in the measurement of the thickness of the non-magnetic coating of core-shell magnetic NPs. As a verification of the effectiveness of the technique we carried out a preliminary analysis on two Fe$_3$O$_4$ and two Cu-coated Fe$_3$O$_4$ NPs. The "dipole model" has been used to calculate the thickness of the coating of the core-shell NPs. The coating thickness values obtained presented good agreement with the average values obtained by the statistical analysis carried out by AFM on the two kinds of NPs. Nevertheless, further more statistically significant analysis needs to be performed in order to assess the accuracy and the reproducibility of the technique.[4]

Another possible application consists in the measurement of the magnetization curve of single magnetic NPs, by performing in-field CM-MFM measurements.

References

1. Pankhurst Q.A., et al. J Phys App. Phys 2009;42: 224001
2. Angeloni L., et al. AIP Conf Proc 2015;1667: 020010
3. Angeloni L., et al. Sci Rep 2016;6:26293
4. Angeloni L. et al., AIP Conf Proc 2016;1749: 020006

AFM study of amyloid self-assembly

Z. Bednarikova,[1] J. Marek,[1] E. Demjen,[1] J. Kubackova,[1] E. Bystrenova,[2] M. M. Mocanu,[3] Z. Gazova[1]

[1]*Department of Biophysics, Institute of Experimental Physics, Slovak Academy of Sciences, Watsonova 47, Kosice, Slovakia*
[2]*C.N.R.- I.S.M.N., Bologna, Italy*
[3]*Department of Biophysics, "Carola Davila" University of Medicine and Pharmacy, Bucharest, Romania*

Corresponding author: Dr. Z. Gazova (gazova@saske.sk)

Key words: AFM, amyloid, morphology.

Introduction

Formation of non-native conformers of poly/peptides and their subsequent self-assembly into amyloid aggregates is one of the hallmarks of more than 30 amyloid diseases such as Alzheimer's disease or lysozyme systemic amyloidosis. Interestingly, although the amyloid fibrils have similar features, they can differ in morphology, stability and cytotoxicity depending on the conditions of fibrils formation.[1] This polymorphism could be important for understanding the molecular basis and the natural variability of amyloid diseases.

The mechanism of amyloid aggregation is still

poorly understood. Peptide-membrane and peptide-lipid interactions are thought to be crucial in this process[2]. Therefore, we have studied the effect of phospholipid on amyloid aggregation of lysozyme at two concentrations.

Materials and Methods

Atomic Force Microscopy (AFM)

Samples of protein were placed on a freshly cleaved mica surface, let adsorb for 5 min, washed with ultrapure water and left to air dry. Unfiltered AFM images were taken in tapping mode using a Scanning Probe Microscope (Veeco di Innova, Bruker AXS Inc., USA) with an uncoated NCHV cantilever at a scan rate of 0.5 kHz. No smoothing or noise reduction was applied. The image analysis was performed using Gwyddion software.

In vitro amyloid fibrillization of lysozyme

Hen egg white lysozyme amyloid fibrils (LAF) were prepared through the incubation of lysozyme for 2 h at 65°C with constant stirring (1200 rpm) (i) in acidic (pH 2.7 - LAF2) and neutral (pH6.0 - LAF6) conditions or (ii) in the presence of phospholipid DMPC (1,2-dimyristoyl-sn-glycero-3-phosphocholine). The formation of fibrillar aggregates was confirmed using Thioflavin T fluorescence assay.

Cell culture

LLC-PK1 (porcine epithelial kidney) cells were grown according to their specifications. 5×10^3 cells/ well in 24 well-plates were incubated in the presence of 0.1, 10 and 100 µg/ml LAF2 or LAF6 for 5 days. The cells were counted using a Bürker-Türk hemacytometer. All experiments were performed in triplicates.

Results and Conclusions

Atomic force microscopy was used to visualize the morphology of the obtained lysozyme fibrils. LAF2 and LAF6 formed fibrils with features typical for amyloid species; however, the morphology was significantly different (Figure 1A). LAF2 represent long fibrillar structures, whereas LAF6 were thicker and shorter and showed a strong tendency to lateral association. The morphology of lysozyme assemblies was determined in more detail by extracting further information about the height, diameter and length of fibrils from the AFM images and respective distribution functions are presented in Figure 1B. The image analysis has shown that the LAF2 fibrils are fiber-like objects with average heights of 6 nm, average length of 955 nm and the average diameter of 7 nm. In con-

trast, the LAF6 fibrils self-assembled into large bundles of fibrils with average heights of 53 nm. It was not possible to obtain the average length and diameter of LAF6 fibrils due to their lateral association and interfibrillar interactions.
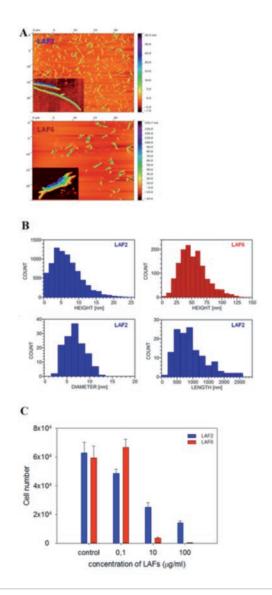

Figure 1. (A) AFM images of LAF 2 and LAF6 in the spectral palette prepared with Gwyddion software. Their 3D details are shown as insets; (B) The distribution function of height, diameter and length of LAF2 (blue) and LAF6 (red); (C) cytotoxic effect of LAF2 (blue) and LAF6 (red) on LLC-PK1 cell line after 5 days.

The morphologically different LAFs also inhibited growth of renal LLC-PK1 cells. Figure 1C illustrates that LAF6 were more toxic than LAF2 at higher concentrations (10 and 100 µg/mL) and at longer incubation time. Our findings indicate that protein aggregation can give rise to fibrillar

species with different degrees of cytotoxicity due to intrinsic differences in pathways of fibrils formation resulting from a formation of various partially unfolded species at the beginning of the process. The influence of DMPC phospholipid on the lysozyme fibrillization was also investigated by AFM to directly visualize their inhibitory abilities. Representative AFM images are presented in Figure 2. The incubation of DMPC with lysozyme led to extensive reduction of the overall amount of the fibrillar structures compare to untreated lysozyme. The fibril/background ratios calculated from AFM images confirmed concentration-dependent inhibitory effect of DMPC - low concentration (40 µM) decreases amount of fibrils to 15.5% whereas 500 µM leads to reduction of fibrils to 0.34% of image area.
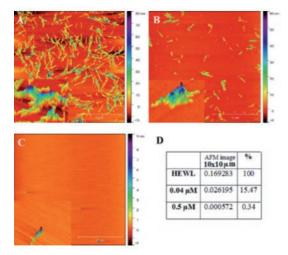

Figure 2. AFM images obtained for lysozyme amyloid fibrils formed alone (A) or in presence of DMPC at 40 µM (B) and (C) 500 µM concentrations. Bars represent 4 µm. (D) fibril/background ratios were calculated using Otsu method in Gwyddion software.

These results have shown that AFM is a very useful tool for a direct observation of amyloid aggregates, their morphological properties and the process of amyloid aggregation in general.

Acknowledgments

References

1. Mossuto M.F., et al. J Mol Biol 2010;402:783
2. Griffin M.D.W., et al. J Mol Biol 2008;375:240

A new scanning probe microscopy standard based on diblock copolymers and holey silicon

F. Ferrarese Lupi,[1] G. Aprile,[1,4] M. Dialameh,[1] N. De Leo,[1] G. Zuccheri,[2] T.J. Giammaria,[3,4] M. Perego,[3] M. Laus,[4] J. Garnaes,[5] L. Boarino[1]

[1]Nanoscience and Materials Division, Istituto Nazionale di Ricerca Metrologica, Strada delle Cacce 91, Torino, 10135, Italy
[2]Dipartimento di Farmacia e Biotecnologie, INSTM, Centro S3, CNR-Istituto Nanoscienze, Via Irnerio 48, Bologna 40126, Italy
[3]Laboratorio MDM, IMM-CNR, Via C. Olivetti 2, 20864 Agrate Brianza, Italy
[4]Dipartimento di Scienze e Innovazione Tecnologica (DISIT), Università del Piemonte Orientale "A. Avogadro", INSTM, UdR Alessandria, Viale T. Michel 11, 1512 Alessandria, Italy
[5]Danish Fundamental Metrology, 307 Matematiktorvet, DK-2800 Kgs. Lyngby, Denmark

Corresponding author: Dr. L. Boarino (l.boarino@inrim.it)

Key words: Length Standard, SPM, AFM, Self Assembly, Diblock Copolymers

Introduction

The direct self-assembly (DSA) of diblock copolymers (DBCs) is widely used as patterning and nanofabrication technique, combining the top-down and bottom-up approaches to the DBC capability of phase separate into the small size and high-density features of different shape. These characteristics suggest the possibility of using the DBCs in order to address the gap in nano-structured lateral standards for nanometrology, consequently supporting the miniaturization processes involved in the semiconductor industry and in nanostructured device fabrication. In this frame, we systematically studied the orientation and ordering process of cylinder forming PS-*b*-PMMA DBC patterns confined within periodic trenches and the variation of its characteristic dimensions (i.e. center-to-center distance L_0 and diameter d) after their propagation into the Si, obtained by means of reactive ion etching (RIE).

Materials and Methods

The self-assembly (SA) of DiBlock Copolymers (DBC) based on the phase separation into different morphologies of small size and high-density features is widely investigated as patterning and nanofabrication technique.[1-3] The integration of the conventional top-down approaches with the bottom-up SA of DBC discloses the possibility to address the lacking of lateral length standards for nanometrology, consequently supporting the miniaturization processes in device fabrication. In
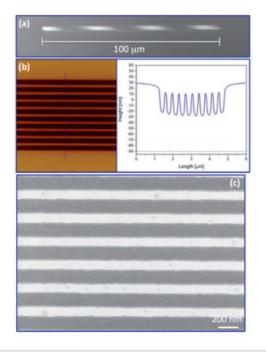
particular, these characteristics suggest the possibility to use DBCs films as organic template to promote the realization of a silicon lateral standard for Atomic Force Microscopy (AFM) calibration in the length scale ranging from 10 nm to 70 nm. In this frame, we studied the DBC behavior when confined within periodic SiO_2 trenches of different width (W, ranging between 75 and 600 nm) and fixed length (L, 5 µm) through a Rapid Thermal Processing (RTP) machine.[4] On one hand, we systematically studied the variation of the characteristic dimension (*i.e.* center-to-center distance L_0) of cylinder forming PS-*b*-PMMA (54 kg mol^{-1}, Styrene fraction 70%) DBC patterns, and on the other hand, we evaluated incidence of confined film thickness on the BCP domain orientation and morphology by varying the process parameters (annealing time and temperature, trench features).
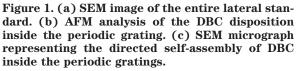
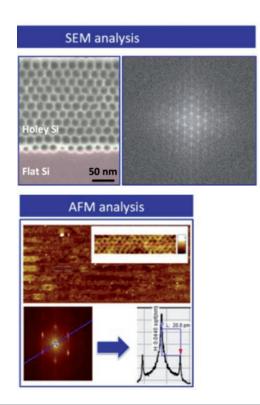## Experimental Results and Conclusion
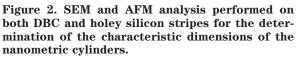
DBC disposition inside periodic trenches

The layout of the lateral standard consists in periodic gratings of ten trenches defined by conventional top down approaches and subsequently neutralized using a P(S-r-MMA) random copolymer (RCP). When the ordering process is accomplished on a flat surface, in a temperature range between 180 and 250°C, cylindrical microdomains perpendicularly oriented with respect to the substrate are observed irrespective of annealing temperature. In contrast, when the ordering process occurs on topographically patterned substrates, different phenomena have to be considered.[5]

The study of the DBC disposition inside the periodic trenches is a fundamental step in the realization of the holey silicon stripes, since it strongly affects the pattern transfer into the Si substrate. Indeed, the simultaneous effect of the flow around the gratings and the DBC flux from the zone located between adjacent trenches (mesa) into the inner part of the trenches results in significant thickness variations of the confined DBC film. Therefore, the amount of DBC inside the trenches depends on the width of the mesa region, which acts as a DBC reservoir. Moreover within each trench group, the DBC thickness progressively decreases from the external to the central trenches composing the periodic grating. The thickness variation of the DBC film within the trenches influences the ordering process, ultimately leading to different orientation of the microdomains in the periodic grating.[6]

Figure 1. (a) SEM image of the entire lateral standard. (b) AFM analysis of the DBC disposition inside the periodic grating. (c) SEM micrograph representing the directed self-assembly of DBC inside the periodic gratings.

Figure 2. SEM and AFM analysis performed on both DBC and holey silicon stripes for the determination of the characteristic dimensions of the nanometric cylinders.

In particular only in a small range of temperatures a precise confinement of the DBC within the trenches featuring a perpendicular cylinder morphology is observed. At higher temperatures mixed or parallel orientations of the microdomains are obtained depending on the width of the trenches composing the periodic grating

Definition of the holey silicon stripes

After the optimization of the DBC ordering inside the periodic trenches, the nanopatterned stripes were transferred into the Silicon layer by means of Reactive Ion Etching (RIE) with two different methods. In the first approach, pattern transfer has been done directly on Silicon by means of Plasmalab 100 and using cryogenic mixing mode of SF_6/O_2 gases. The second approach is using hard mask of SiO_2, in which pattern transfer into the SiO_2 has been performed in Plasmalab 80 Plus by using CHF_3/Ar gases. For Silicon etch step, Pseudo Bosch process (SF_6/C_4F_8) has been adopted and performed again by Plasmalab 100.

Finally, in order to determine the exact values of the geometrical parameters of the confined nanodomains, SEM and AFM analysis have been systematically performed on the holey silicon stripes and compared with that obtained on the flat surface.

The object of this was to develop the first prototype of lateral standard for SPM traceable calibration based on holey silicon. The standard have been developed using the self-assembly properties of DBCs with tunable characteristic dimensions between 13 nm and 50 nm.

References

1. Black C. T. et al. IBM J Res & Dev 2007;51:5
2. Kim S. O. et al. Chem Rev 2010;110:146-77
3. Darling S. B., Prog Polym Sci 2007;32:1152
4. Ferrarese Lupi F. et al, Nanotechnology 2013; 24:315601
5. Ferrarese Lupi F. et al. J Mater Chem C 2014; 2:2175-82.
6. Ferrarese Lupi F., et al. ACS Appl Mater Interfaces 2015;7(42):23615-22.

Measurement of magnetic vortex chirality by field-dependent local hysteresis loops with MFM

M. Coïsson, G. Barrera, F. Celegato, A. Manzin, P. Tiberto

INRIM, strada delle Cacce 91, 10135, Torino, Italy

Corresponding author: Dr. M. Coïsson
(m.coisson@inrim.it)

Key words: MFM, magnetic vortices, chirality.

Introduction

Magnetic patterned media are considered interesting materials for a variety of applications, including magnetic storage and microwave oscillators.[1] In the form of dots with suitable thickness to diameter ratio, magnetic vortices can be formed which can be exploited to permanently store information, coded in the vortex chirality. Many techniques for imposing a chirality in magnetic dots are available, which include rotating field or field impulses, suitable tailoring of the dots shape to break their symmetry, and many-body interactions. For reading the vortex chirality, X-ray magnetic circular dichroism, SEM with polarization analysis, planar Hall effect, magneto-resistance, Lorentz Effect TEM are very powerful yet extremely complex experimental techniques.

Magnetic force microscopy (MFM) is relatively common and extremely effective for this purpose. In this paper, we will briefly show how MFM can be used to investigate the formation of the vortex chirality in magnetic dots.[2] Besides the usual approach of collecting MFM images at different applied magnetic field values, field-dependent MFM techniques have been recently developed that allow the measurement of local hysteresis loops in individual patterned structures.[3,4] Common measurement and modelling tools do not offer sensitivity on the vortex chirality, because magnetic hysteresis loops are normally degenerate with respect to it. Conversely, in this paper we will show that local hysteresis loops measured by MFM are able to distinguish between chirality states and offer a means of studying more effectively the magnetization reversal processes in magnetic dots.

Materials and Methods

$Ni_{80}Fe_{20}$ dots with a thickness of 30 nm have been prepared by sputtering on SiO_2 substrates using electron beam lithography. The lateral size of the dots is of approximately 800 nm. The dots

are arranged in a square array where individual elements are spaced by more than 2 μm in order to minimize magnetostatic interactions.

Local hysteresis loops have been measured by means of Magnetic Force Microscopy (MFM, Bruker Multimode V Nanoscope 8 equipped with a fully non magnetic head and scanner) using a recently developed technique,[2,3] consisting in disabling the slow scan axis of the microscope while synchronizing the magnetic field variations with the end of line signal. As a result, an image consisting of phase, pass 2 lines of the same profile acquired each at a different applied field value is obtained. Arbitrary magnetic field histories can be generated. Each image contains therefore the information on the evolution of the magnetization under the application of a magnetic field which can assume several hundreds or even thousands different values. A suitable image analysis can reveal the local hysteresis loops irreversible features and provide details on the magnetization reversal of micrometric and sub-micrometric structures. The equilibrium configuration of the magnetization has also been calculated using micromagnetic simulations; then, the corresponding MFM images have been reconstructed by assuming a tip uniformly magnetized along the vertical axis and not affected by the stray field of the sample or by the applied magnetic field.[2]

Results and Conclusions

Figure 1 reports the four possible evolutions of the magnetization of a dot submitted to a magnetic field that cycles from positive to negative saturation and back. On the left of the figure, the MFM images reconstructed from the micromagnetic simulations are reported, together with the corresponding local hysteresis loops.[2] Even though the images look quite similar, their detailed analysis reveals four different cases, leading to significantly different local hysteresis loops. The four cases correspond to the relative position of the MFM scan line and of the edge along which vortex nucleation and expulsion occurs. In particular, type I and II loops correspond to vortices nucleating along the same edge of the dot both in the first and second loop branch (which means that the chirality is inverted in the two branches), with the tip scanning respectively close to the opposite and same edge. Type III and IV loops correspond to vortices nucleating along opposite edges of the dot in the first and second loop branch (which means that the chirality is preserved in the two branches), again for the two different positions of the tip scan line.

The comparison with the experimental data (right side of Figure 1) reveals a striking agreement with the simulations, both in terms of appearance of the MFM images, and especially concerning the local hysteresis loops shape, where the branches relative disposition, cross points and main features perfectly match. Type I loops are notably missing from the collected experimental data, whereas type II loops turn out to be observed most of the time. A careful investigation of the tip-sample interaction has been performed,[2] revealing the influence of the tip in inducing the nucleation side of the vortex and therefore the probability of appearance of the different loop types.

In conclusion, the proposed field-dependent MFM technique can be exploited to both measure and control magnetic vortex chirality in patterned dots. The validity of the technique has been tested experimentally and by comparison with numerical results.
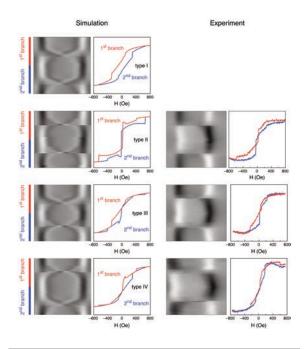

Figure 1. Comparison between simulated (left) and experimental (right) MFM images, and corresponding local hysteresis loops, of a $Ni_{80}Fe_{20}$ square dot submitted to an in-plane magnetic field.

References

1. Bader S.D. Rev Mod Phys 2006:78:1
2. Coïsson M., et al. Sci Rep 2016:6:29904
3. Coïsson M., et al. J Phys D: Appl Phys 2014:47:325003
4. Coïsson M,. et al. Microscopie 2014:marzo:23

A combined STM and optical investigation of the solid-liquid interface

L. Fazi, B. Bonanni, C. Goletti

Physics Department, University of Rome "Tor Vergata", Rome, 00133, Italy

Corresponding author: L. Fazi (fazi@roma2.infn.it)

Key words: Scanning probe microscopy, reflectance anisotropy spectroscopy, solid-liquid interface.

Introduction

The use of scanning probe microscopy (SPM) to investigate low dimensional systems represents the most common and standard characterization of surfaces, interfaces or more generally nanostructures. Furthermore, the possibility of coupling SPM with different spectroscopies often opens larger perspectives, to solve long-standing scientific issues. In this article we present two significant examples of how SPM can be combined with optical spectroscopy, to investigate: i) a complex case of reconstructed surface in Ultra High Vacuum (UHV) and ii) a liquid/solid interface.

Materials and Methods

In both examples we exploit the versatility of a particular surface-sensitive optical technique, reflectance anisotropy spectroscopy (RAS), and the unsurpassed spatial resolution of STM.

Reflectance anisotropy spectroscopy (RAS) mimics ellipsometry at normal incidence, measuring the anisotropy of light linearly polarized along two orthogonal directions of the sample surface.[1] It is a surface sensitive optical technique, non-destructive (using low energy photons, in the range 300-800 nm), and can be applied in UHV, liquid and air. The signal is averaged on the light spot size (2-3 mm^2), and can also provide information from the buried interface (within the penetration length of light). The STM experiments were performed in UHV by a commercial VT-STM Omicron, and in liquid by a home-made instrument able to investigate the solid/liquid interface of a sample immersed in an electrochemical cell.[2] Cyclic voltammetry data can be acquired in situ on the same sample.

Results and Conclusions

Ge/Si (105) surfaces exhibit a complex strained reconstruction known as rebounded-step (RS),[3] where the subsurface layer, hidden from probe microscopy, has a key role to determine electronics and optical properties of the entire recon-

struction. At different values of the Ge coverage, STM images (left panel of Figure 1) show that the zig-zag motif typical of RS is always clearly present, while defects density changes. On the contrary, RAS spectra (central panel) have a well-marked dependence upon the surface preparation stage. Density Functional Theory (DFT) results (right panel) confirm the experiments and explain how the spectral line-shape depends upon the stoichiometry below the topmost layer of the surface, producing true surface states inside the bulk band gap.[4]
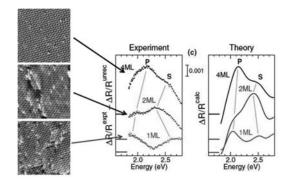

Figure 1. STM images (50 x 50 Å^2) of the (105) surface for increasing coverage θ of Ge and corresponding measured RAS spectra (central panel) for the same coverage values. Computed RAS spectra are also compared (right panel). Lines are a guide for the eye.

When it is used to study surfaces immersed in liquid, RAS allows to investigate the surface–liquid interface in situ and in real time during the evolution of reactions at particular surfaces or in specific reagents.[2,5] Electrochemical Scanning Tunnelling Microscope (EC-STM) is also well suited for liquids. In Figure 2, STM images of a Cu(110) surface in hydrochloric acid solution are presented at selected values of the electric potential applied to the metal sample in an electrochemical cell.[2] The evident unidirectional stripes are due to adsorption of chlorine on the copper surface. The RAS signal recorded at fixed wavelength (corresponding to the peak of the chlorine stripes-related anisotropy, at 2.5 eV) is then measured during the cyclic variation of the electric potential. Once correlated with the STM images acquired during the same cycle, it provides a fast response to monitor in real time the surface modification. The obtained curve (Figure 2), signifying the modification of the RAS signal (RAS) with respect to the clean copper surface, represents the time evolution of the adsorption/desorption of chlorine.

We believe this approach will provide meaningful developments in particular for the solid/liquid interface, where the incompatibility of normally used surface probes (often restricted to UHV) with liquid still represents a significant limit for investigation.
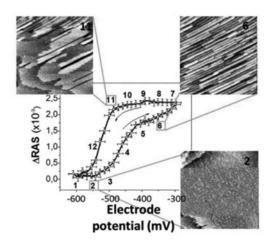

Figure 2. Evolution (at fixed photon energy, 2.5 eV) of the optical anisotropy signal ΔRAS as a function of the sample potential for the Cu(110) surface in HCl solution. STM images (81 nm2) acquired at selected potential values are reported. The arrows inside the cycle indicate the scan direction of the potential (positive and negative directions). The numbers represent the potential value at which STM pictures have been acquired in liquid. Some images are reported: (2) clean copper surface, (6) stripes of adsorbed chloride running along the [0 0 1] direction of the surface, and (11) copper terraces reappearing after partial desorption of chloride (channels due to chlorine are clearly evident).

References

1. Weightman P., et al. Rep Prog Phys 2005;68: 1251.
2. Goletti C. et al. Phys Chem C 2014;1782-1790: 119 and references therein
3. Persichetti L., et al. Phys Rev Lett 2010;104: 036104
4. Fazi L., et al. Phys Rev. B 2013; 88:195312 and references therein
5. Barati G., et al. Langmuir 2014; 30:14486-93.

Characterization of electrical nano-scale properties of Si-based thin films for photovoltaic applications

M.A. Fazio,[1] M. Perani,[1] N. Brinkmann,[2] B. Terheiden,[2] D. Cavalcoli[1]

[1]Department of Physics and Astronomy, University of Bologna, viale C. Berti Pichat 6/II, 40127 Bologna, Italy
[2]Department of Physics, University of Konstanz, Universitaetstrasse 10, D-78464 Konstanz, Germany

Corresponding author: M. A. Fazio
(maria.fazio2@unibo.it)

Key words: conductive AFM, photovoltaic, silicon oxy-nitride.

Introduction

Actual research on solar cells is focused on efficiency improving, as well as cost reduction and optimization of production processes feasible at commercial and industrial scale. Within this perspective, silicon heterojunction (SHJ) solar cells with thin films were produced, following a multijunction concept, with a record efficiency of 25.6% in 2014.[1,2]

In SHJ solar cells, a doped amorphous silicon layer (a-Si:H) is deposited on top of the crystalline silicon (c-Si) active material, to create the electric field of the pn junction, with the addition of passivation layers to avoid surface recombination.[1] Notwithstanding the good passivation qualities of a-Si:H, carriers with short lifetime are generated in this material and a large fraction of them recombine, causing a high parasitic light absorption.[3] Within thin films solar cells technology, silicon oxy-nitride (SiO_xN_y) turns out to be a promising material as a substitute for a-Si:H, for its tunable large bandgap and high conductivity (up to 2.5 eV and 44 S/cm), as well as its low contact resistance with the transparent conductive oxide.[3] Our previous studies have shown that the physical properties of the SiO_xN_y layers are affected by both nitrous oxide dilution and thermal treatment, due to different O inclusion and relocation.[4,5] These parameters cause a variation in crystalline fraction of the layers, their macroscopic electrical conductivity and morphological properties at the nanoscale[4,5]

Conductive Atomic Force Microscopy (c-AFM) is a useful non-destructive and cheap technique, to study nanometric electrical properties of complex samples with several phases. It consists of a conductive tip put in contact with the sample surface, while the current flow between them is measured at constant bias.

In the present contribution, c-AFM technique

has been used to study the electrical properties at the nanoscale of B doped silicon oxy-nitride deposited with different parameters, to extract a model of electrical conduction in these materials.

Materials and Methods

P-type SiO_xN_y layers (nc-SiO_xN_y) are deposited by Plasma Enhanced Chemical Vapor Deposition (PECVD) on FZ-Si substrate. Silane (SiH_4), hydrogen (H_2) and nitrous oxide (N_2O) are used as precursor gases, with diborane (B_2H_6) diluted in hydrogen (0.5%) to achieve p-type doping. The deposition temperature is 300°C and the radio frequency (RF) is set at 13.56 MHz. The flow of N_2O and the ratio of B_2H_6 are both referred to their dilution in silane. The samples are deposited with a fixed diborane dilution (2.34%) and then annealed at 800°C in a nitrogen atmosphere to promote nanocrystals formation.

The investigated samples are selected by changing only one deposition parameter each time: N_2O dilution (R) and annealing (TT), respectively. This choice is made to show how the change in the parameter affects the nanometric electrical properties of the samples. The analyzed samples are the following: A (R=9.09%, TT=0 h), B (R=9.09%, TT=3 h), C (R=47.4%, TT=3 h), with thickness in the range of 200 nm. It has to be noted that higher values of R correspond to a higher O content within the layers, causing a lower crystalline fraction and a macroscopic electrical conductivity decrease.[3,4]

C-AFM acquisitions are performed using a Park NX10 system in contact mode with Pt probe, with nominal tip radius smaller than 20 nm. A fixed bias is applied to the sample through the silver paste contact on the top side of the sample, while the current is extracted from the tip.

Results and Conclusions

Current maps of 1x1 μm^2 have been recorded in several fresh areas of the nc-SiO_xN_y layers. As an example, a map on sample A is reported in Figure 1a. The dark areas in the image correspond to conductive regions of the sample. Grain-like structures in a low conductive matrix are visible on the surface of all the samples, however the grain conductivity is affected by annealing time and oxygen content. In sample B, the high conductive grains agglomerate forming clusters; this effect is in accordance with the observed coalescence and clustering of nanocrystals and the O relocation.[4] Moreover, sample B shows the highest conductance at the nanoscale, since both annealing and low O content promote electrical transport. In

addition, it is the only sample that show enhanced conductance at positive biases, due to holes' conduction. This means that low O content promotes B-dopant activation in p-type layers.
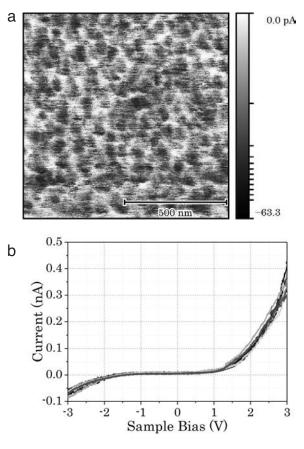

Figure 1. (a) Current AFM map on sample A at negative bias (-1.5 V); a non-linear scale is used. (b) Example of several I-V characteristics on sample A with a linear change in bias ([-3, 3] V).

Current-voltage (IV) characteristics have been measured locally on high conductive points (grains) of sample A (Figure 1 b). The tip-sample junction can be described as a Schottky contact, so the IV curves are well fitted by a thermionic emission theory, in accordance with the fact that the barrier of the highest conductive sample is the lowest one.

C-AFM analyses of microscopic transport properties of nc-SiO_xN_y thin films for photovoltaic applications have demonstrated that different deposition parameters (annealing, O concentration) strongly affect nanoscale electrical properties; in particular, low O content promotes B activation in p-type samples. Conductive AFM has demonstrated to be a very useful tool for the study of these multi-phase and non-stoichiometric thin films.

References

1. DeWolf S., et al. Green 2012;2:7
2. http://news.panasonic.com/press/news/official.data/data.dir/2014/04/en140410-4/en140410-4.html, 2014
3. Brinkmann N., et al. Sol Energ Mat Sol C. 2013;108:180
4. Perani M., et al. J Phys Chem C. 2015;119:13907
5. Perani M., et al. Thin Solid Films 2016;DOI: 10.1016/j.tsf.2016.03.067

Surface roughness in Al-implanted 4H-SiC substrates for different Al concentrations and after 1950°C post implantation annealing

P. Fedeli,[1] C. Albonetti,[2] R. Nipoti[1]

[1]IMM-CNR, via Gobetti 101, 40129 Bologna, Italy
[2]ISMM-CNR, via Gobetti 101, 40129 Bologna, Italy

Corresponding author: Dr. P. Fedeli
(fedeli@bo.imm.cnr.it)

Key words: 4H-SiC, Al doping, ion implantation

Introduction

Silicon carbide (SiC) is a wide bandgap semiconductor suitable to fabricate low-loss, high-power and high-frequency devices for harsh environments. Selective area doping by ion implantation is often used in the fabrication of SiC electronic devices. To obtain p-type regions the preferred dopant species is aluminum (Al), that can be implanted on a wide concentrations range (from 10^{17} to 2×10^{20} cm^{-3}) with an accurate spatial distribution. After the implantation, a high-temperature (up to 1950°C) post implantation annealing is required to recover the lattice disorder produced by ion bombarding and electrically activate the implanted impurities. However, during such treatments a surface degradation of SiC is usually observed and the mirror-like surface is completely lost, due to Si desorption and atom migration on the surface.[1] This is a problem both for device fabrication and for material properties investigation, as the conditions required for a proper optoelectronic characterization are not fulfilled if the SiC surface is too rough. Proper SiC surface capping during the post-implantation annealing effectively suppresses the roughening phenomenon and, among the several capping materials proposed in the last years, a thin carbon layer (C-cap) gives the most successful results.[2]

In this study the surface roughness of Al-implanted on-axis 4H-SiC substrate is investigated by Atomic Force Microscopy (AFM) for implanted Al concentrations in the range $5\times10^{18} - 1.6\times10^{20}$ cm^{-3} after a 1950°C/12 min annealing with C-cap.

Materials and Methods

A High Purity Semi-Insulating (HPSI) on-axis <0001> 4H-SiC wafer was Al$^+$ implanted by using a Tandentron 1.7 MV accelerator (High Voltage Engineering Europa B.V.). Different ion energies and ion doses were used so to obtain implanted Al depth profiles of almost box shape next to the surface with fixed 400 nm thickness but different plateau heights in the range $5\times10^{18} - 1.6\times10^{20}$ cm^{-3} on different pieces of the same SiC wafer. After the implantation, a resist film was spun on the implanted surface of each piece and transformed in a carbon layer (C-cap) by a pyrolysis at 900°C for 2 min in forming gas.[3]

Post implantation annealing processes were performed in a conventional inductively heated furnace in high purity Ar atmosphere (for a comprehensive description of the annealing system, see ref. [4]) at 1950°C for 12 min. The same heating and cooling transients were used for all the samples.

After annealing, the C-cap was removed from the samples surface by a 850°C/15 min dry oxidation process. The surface morphology of the as-implanted and of the annealed samples after C-cap removal was characterized by atomic force microscopy (AFM) in contact and non-contact mode, respectively. The surface morphology of the samples was evaluated by measuring the root-mean-square (RMS) roughness over an area of 10 μm × 10 μm and 5 μm × 5 μm for the annealed and virgin samples, respectively.

Results and Conclusions

Figure 1 shows the surface morphology of a 4H-SiC sample implanted by an Al concentration of 1.6×10^{20} cm^{-3} before and after the post implantation annealing. The RMS roughness of the virgin and annealed samples are 0.39±0.04 and 0.56±0.08 nm, respectively. The AFM image of the annealed sample shows the formation on the surface of few nanometer deep circular pits with a diameter of ≈ 1 μm (Figure 1b). A similar morphology is observed in the annealed samples implanted by the other Al concentration values of this study, not shown in Figure 1. No significant dependence of the surface roughness on the implanted Al ion dose was observed, as shown in Figure 2. Similar trend was previously reported for P-implanted 4H-SiC.[5] With the exclusion of the 5×10^{19} cm^{-3} sample (presently considered a scattered point), the ave-

rage RMS roughness for the implanted concentrations is (0.57±0.2) nm, that is comparable with the RMS roughness before annealing and highly acceptable for microelectronic device fabrication. These results show the high quality of the C-cap used in this study, which can withstand annealing temperatures up to 1950°C.
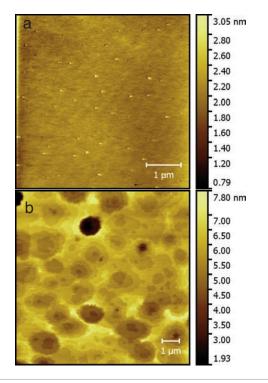

Figure 1. AFM images of the same $1.6×10^{20}$ cm^{-3} Al+ implanted 4H-SiC sample before (a) and after (b) the 1950 °C/12 min post implantation annealing with C-cap (removed before AFM measurements).
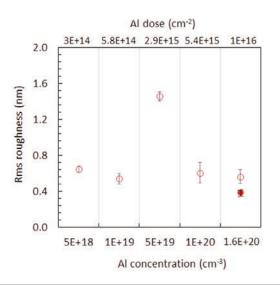

Figure 2. RMS of 4H-SiC samples versus implanted Al concentration (Al dose): (●) as-implanted, (○) after post implantation annealing.

References

1. Kimoto T., Cooper J.A. in "Fundamentals of Silicon Carbide Technology", John Wiley & Sons ed., 2014, p. 202
2. Negoro Y., et al. J Appl Phys 2004;96:224
3. Nipoti R., et al. Electrochem Solid-State Lett 2010;13:H432.
4. Fedeli P., et al. ECS J Solid-State Sci Technol 2016;5:P534.
5. Nipoti R., et al. J Electron Mater 2010;41:457.

Effect of an antimicrobial peptide on model membranes studied by Atomic Force Microscopy and Fluorescence Microscopy

N. Marín-Medina,[1] A. Alessandrini[2,3]

[1]Department of Physics, University of Los Andes, Carrera 1 N° 18A - 12, Bogota, Colombia
[2]Department of Physics, Informatics and Mathematics, University of Modena and Reggio Emilia, Via Campi 213/A, 41125, Modena, Italy
[3]CNR-Nanoscience Institute-S3, Via Campi 213/A, 41125, Modena, Italy

Corresponding author: N. Marín-Medina (nmarin@uniandes.edu.co)

Key words: antimicrobial peptides, Atomic Force Microscopy, Fluorescence Microscopy.

Introduction

Antimicrobial peptides (AMPs) are small amphipathic molecules produced in plants and animals to fight bacterial infections. Magainin, a 23-residue peptide secreted by the skin of an African frog, is a classical and widely studied α-helical AMP.

The proposed mechanism of action of AMPs suggests, at low peptide-to-lipid ratios, a lateral expansion of the lipid membrane due to peptide surface binding.[1] The lateral expansion induces a corresponding membrane thinning due to the almost constant volume of lipid bilayers.

Studies have shown that magainin binding causes membrane thinning[2] and softening.[3] In particular, Atomic Force Microscopy (AFM) studies showed membrane thinning due to a magainin analog, MSI-78.[4] However, the study of the effect of exogenous molecules on Supported Lipid

Bilayers (SLBs), the model system usually studied by AFM and considered 'at constant area', could provide different results with respect to freely suspended liposomes, a model considered 'at constant lateral tension'. Here, we used AFM-based force spectroscopy to measure the force required to punch through the membrane, and Fluorescence Microscopy to observe the effects of mag-H2 binding on SLBs composed of PalmitoylOleoylPhosphatidylCholine (POPC). The measurements aimed at understanding if the presence of a nearby solid substrate could induce some artifacts on the obtained results for SLBs with respect to liposomes.

Materials and Methods

POPC, solubilized in chloroform, was mixed with 1% molar DHPE-Texas Red and used to prepare Giant Unilamellar Vesicles (GUVs) by the electroformation method in 100 mM sucrose solution. In a homemade chamber with mica as the bottom surface, GUVs were deposited in 105 mM glucose, and then ruptured by adding 1-3 drops of a concentrated $MgCl_2$ solution to obtain lipid bilayer patches on the surface. The glucose solution was then replaced with the imaging buffer (150 mM KCl, 8 mM Hepes, 3 mM $CaCl_2$, pH 7). Fluorescent images were acquired with an inverted optical microscope (Olympus IX70). AFM force curves (tip speed: 1 µm/s; nominal spring constant: 0.24 N/m) were acquired with a Bioscope I microscope equipped with a Nanoscope IIIA controller. The peptide mag-H2 was hydrated in Millipore water and diluted to the desired concentration. The reported mag-H2 concentrations indicate the final concentrations in solution.

Results and Conclusions

For force spectroscopy analysis, lipid bilayer patches with no lipids on top were considered. The bilayer was exposed to concentrations of 0, 1.5 and 3 µM mag-H2. The area of the patch, obtained from fluorescence images, exhibited a significant increase at 3 µM. When taking force curves on this patch, we observed the clear presence of a jump-through event only at 0 and 1.5 µM (Figure 1). Apparently, at 3 µM, where a large lateral expansion had occurred, the structure of the membrane was already compromised so that there were not the conditions to obtain a clear jump through event. The most probable jumpthrough force increased from 2.3 nN at 0 µM to 4.5 nN at 1.5 µM, suggesting a stiffening of the membrane. When considering liposomes, it has been found that magainin typically induces a softening of the lipid bilayer.[3]
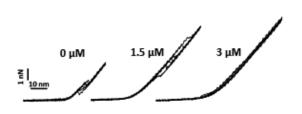

Figure 1. Representative force curves for a POPC bilayer exposed to three different mag-H2 concentrations.

We also studied a patch, 200 µm in diameter, with some small patches on top, using only Fluorescence Microscopy (Figure 2). This sample was exposed to a 20 µM mag-H2 concentration. Just after adding the peptide, lipid tubes began to form from the surface of the patch. After 60 seconds of peptide exposition, the area of the patch began to increase reaching a final 5% total area variation (Figure 2c). In contrast, one of the small patches on top, ~2 µm in diameter (see inset to Figures 2a and 2b), began to laterally grow immediately after adding the peptide, reaching a final 300% total area variation. These results suggest a strong interaction between the SLB and the mica surface which restricts the lateral expansion of the membrane. The accumulated tension due to peptide binding is released through the formation of lipid tubes, while for the patch over the SLB, the lateral expansion has no restrictions.

We conclude that the surface under the SLB affects significantly the effects of mag-H2 binding. This could lead to different results when comparing with studies using other model membranes.
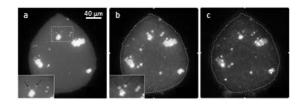

Figure 2. a) a POPC patch on mica before the injection of mag-H2 peptide. The inset is a magnification of the rectangular area shown by a dashed white border; b) The same patch after been exposed to a 20 µM mag-H2 concentration for 60 s. The inset is the same as in a). The dashed white line represents the border of the patch in a); c) The same patch after 200 s. The dashed line is again the border of the patch in a).

Acknowledgments

———————

References

1. Lee M., et al. Proc Natl Acad Sci 2008;105:5087
2. Ludtke S., et al. Biochemistry (Mosc) 1995;34:16764
3. Bouvrais H., et al. Biophys Chem 2008;137:7
4. Mecke A., et al. Biophys J 2005;89:4043

Hydroxy-silicate substrates for biomolecules characterization

D. Moro, G. Valdrè

Centro di Ricerca Interdisciplinare di Biomineralogia, Cristallografia e Biomateriali
Dipartimento di Scienze Biologiche, Geologiche e Ambientali, Università di Bologna, Piazza di Porta San Donato 1, 40126 Bologna, Italy

Corresponding authors:
Prof. G. Valdrè (giovanni.valdre@unibo.it)
Dr. D. Moro (daniele.moro@unibo.it),

Key words: substrates, nanolithography, single biomolecules.

Introduction

The ability to confine the deposition of single biomolecules onto specific nanosized areas is a requirement of paramount importance for their characterization. The substrate should be reasonably flat, homogeneous and chemically stable. Common ways of patterning surfaces make use of self-assembly of molecules combined with nanolithography. AFM nanolithography can be exploited to create nanosized areas with a specific chemical affinity onto an inert and uniform surface for bionanopatterning; then the molecules of interest will be deposited on these surfaces and will bind specifically on the patterned areas. Most of the substrates are not atomically flat, are chemically uniform across the surface and requires time consuming preparation procedures.

In this work we show that, by taking into account the crystal chemistry and surface potential properties of a magnesium–aluminum hydroxide–silicate substrate it is possible to perform well-controlled removal of the sub-nanometer thick structural layers of the substrate at the nanometer level. Furthermore, the resulting atomically flat and charged pattern is used for effective characterization of biomolecules at the nanometer scale.

Magnesium–aluminum hydroxide–silicate is an electrostatic crystal made up of regularly stacked negatively charged TOT (tetrahedra–octahedra–tetrahedra) mica-like layers, 1 nm thick, sandwiching a positively charged Mg–Al-hydroxide octahedral layer, 0.4 nm thick. The material contains several per cent of Al both in the tetrahedral sites of the TOT substituting silicon and in the hydroxide layer substituting Mg. The double Al substitution confers a positive charge to the hydroxide layer and a negative to the TOT surface. The two layers are bonded to each other by a weak electrostatic force. Once cleaved the material can expose simultaneously regions of the TOT (negative and hydrophilic), and of hydroxyl groups belonging to the hydroxide layer (positive and hydrophobic). The surface potential difference drives the deposition of charged biomolecules.[1-3]

Materials and Methods

The Mg–Al-hydroxide–silicate was prepared and characterized at the Laboratory of Biomaterials and Applied Crystallography of the University of Bologna (Italy). Its composition was previously determined by means of electron microprobe analysis in the wavelength-dispersive mode and the crystal structure by a Bruker X8-Apex fully automated four-circle diffractometer.[1]

A Nanonis SPM control system (Nanonis—SPECS Zurich GmbH, Zurich, Switzerland) equipped with two oscillation controller modules (with digitally integrated PLL/lock-in) and a software lock-in detector module was used for topography measurements, Kelvin probe analysis and nanolithography. The precise control of the relative tip–sample position was achieved by an nPoint closed-loop MultiMode scanner (nPoint, Inc., Madison, WI, USA). Single-pass amplitude-modulation Kelvin probe was used for surface potential measurements.

Results, Discussion and Conclusions

Figure 1 B shows as an example an AFM topographic image of a just prepared surface of the magnesium–aluminum hydroxide–silicate. Bright areas represent the Mg–Al-hydroxide layer, 0.4 nm thick in good agreement with single crystal x-ray diffraction results, extending over the mica-like layer (darker background). Terraces were observed to be atomically flat and extended in size from about 700 nm down to few tens of nm. In general, for this material the surface potential difference between the TOT basal plane (dark areas in Figure 1, B) and the hydroxide layer upper sur-

face (bright areas in Figure 1 B) gave figures, as measured by Kelvin probe force microscopy, ranging from 50 to 500 mV (at room temperature, atmospheric pressure and relative humidity of 30–70%), because of the variable surface crystal chemistry and environmental conditions. Here, these surface potential differences were applied to drive the deposition of single glycine molecules. To this aim AFM nanolithography was used to produce a custom nanopattern. Mechano-voltage nanolithography was performed in contact mode to expose at the surface a wide TOT area (Figure 1 A). Figure 1 A shows the central part of the surface in Figure 1 B after controlled removal of a portion of the 0.4 nm thick hydroxide layer and after deposition of glycine molecules. A specific procedure was developed to investigate the same nanosized area before and after ex situ biomolecules deposition. Single biomolecules (bright dot-like structures) were observed to be preferentially adsorbed in a stable manner onto the hydroxide surface, whereas no stable adsorption was observed onto the mica-like surface.
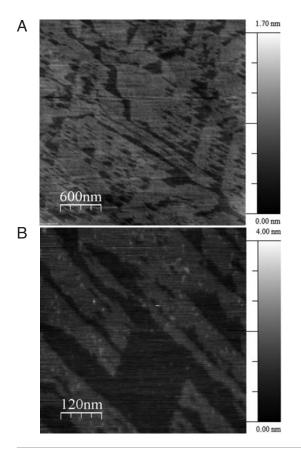

Figure 1. (A) Just prepared surface. (B) After nanolithography and glycine deposition.

This material allows the construction of atomically flat and charged patterns, designed to guide biomolecules deposition and stable adsorption without the need of any chemical functionalization of the surface. It is a promising substrate that could offer unique applications in several areas of bio-nanopatterning and particularly for surface driven deposition of biomolecules. This substrate was also found to be effective in the manipulation of single DNA molecules, single RNA molecules and nucleotides.[1-3] Similar procedures can be readily extended to other charged organic molecules for life science and polymer research, where the exploitation of self-assembled mechanisms on a large scale is in high demand.

References

1. Valdrè G. Eur. J Mineral 2007;19:309
2. Valdrè G., et al. Micro Nano Lett 2011;6:922
3. G. Valdrè, et al. Nanotechnology 2012;23: 385301

Exosomes distribution in cells via X-ray Fluorescence Microscopy

P. Parisse,[1] E. Ambrosetti,[1] D. Mangoni,[2] D. Cesselli,[2] A. P. Beltrami,[2] A. Gianoncelli,[1] L. Casalis[1]

[1]Elettra Sincrotrone Trieste, s.s. 14 km 163.5 in Area Science Park, Trieste, Italy
[2]Department of Medical and Biological Sciences, University of Udine, Udine, Italy

Corresponding author: Dr. P. Parisse (pietro.parisse@elettra.eu)

Key words: Extracellular Vesicles, X-Ray-Fluorescence Microscopy, Atomic Force Microscopy.

Introduction

Exosomes are small vesicles (50-200 nm diameter) released in the extracellular space by most of the mammalian cells and represent one of the major routes of intercellular communication.[1] The content of such vesicles (miRNAs, mRNAs, proteins, etc.) can indeed alter and modulate the response of recipient cells. The ability of exosomes to travel in all body fluids (blood, saliva, urine) allows them to get in contact with cells localized very far from the originating cell, making them one of the main suspects of the elusive mechanisms of metastatic spreading (pre-metastatic niche). In fact, a strong effect has been attributed to exosomes derived from tumour cells in modulating the evolution of tumour microenvi-

ronment itself. This effect has been observed in different classes of tumours (glioblastoma, ovarian cancer, gastric cancer, breast cancer)[2-5] and we have recently shown a prominent role of glioma-derived exosomes in enhancing the aggressiveness of the tumour.[6] Yet, the complexity and heterogeneity of exosome origin and composition and their small size, make structural/functional studies on exosome uptake challenging to many available microscopy techniques. X-Ray Fluorescence Microscopy could have the potential of unravel mechanisms of exosome/cell interactions due to its high chemical sensitivity that can reveal subtle metabolic changes affecting elemental composition inside cells.[7] These details can be resolved within micrometer resolution by exploiting the XRSM, making possible a biochemical profiling of individual cells. Here we present our preliminary results of X-Ray Fluorescence Microscopy to evaluate the distribution of exosomes functionalized with Fe_2CoO_4 nanoparticles (NPs) in glioma cells, with a 500-800 nm lateral resolution.

Materials and Methods

Glioma Associated Stem Cells have been cultured on silicon nitride membranes in the presence or not of exosomes purified from Glioma Cells as reported in ref. 8. In order to monitor the internalization of exosomes by GASC cells, purified vesicles have been labelled with antiCD9 functionalized $CoFe_2O_4$ NPs.[9] After 72 h in culture, unconditioned and conditioned cells have been fixed and dehydrated. We measured 3 types of samples: fixed GASC cells not conditioned (Control); fixed GASC cells conditioned with NPs (NP Control); fixed GASC cells conditioned with NP decorated exosomes (EXONP). Fixed cells have been then imaged by means of XRM and XRF measurements allowing for the mapping of the distribution of exosomes inside the cells.[10] Atomic Force Microscopy images of GASC fixed cells have been acquired with XE-100 instrument (Park Instruments) in contact mode in air. 40x40 μm^2 images at 256/512 pixel per line have been acquired and analysed using XEI (Park Instruments) and Gwyddion softwares.

Results and Conclusions

In Figure 1 we report the Atomic Force Microscopy image of a GASC cell after 72 h exposure to EXONPs, and the corresponding low energy x-ray fluorescence (XRF) maps relative to different elements O, Mg, Co and Fe. O and Mg maps reveal the main structure of the cell (been rather homogeneously distributed in the cells), whereas the Fe and Co maps show the colocalization, sign of presence of NPs, and therefore of the occurred interaction of the Exosomes. The EXO-NPs are present mostly in the cytoplasmatic region, in good agreement with optical fluorescence measurements performed on similar cell cultures.[6] In all the other samples the Co and Fe fluorescence signal was completely absent (Control, not shown here) or sporadically present (NP, not shown here), demonstrating the specific interaction of exosomes with the cells. These preliminary results demonstrated the feasibility of the study of uptake of extracellular vesicles by means of XRF microscopy. Moreover the combination of AFM (real 3D topography) and XRFM could also allow to map the elemental distribution inside the cells and to extract atomic concentrations[7]: this label-free characterization of cells of different origin upon exposure to exosomes could bring to the discovery of new specific fingerprints of exosome interaction.
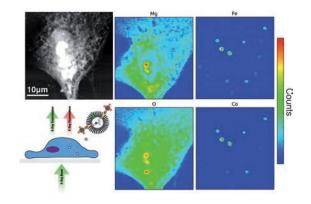

Figure 1. Atomic Force Microscopy topographic image and corresponding elemental maps from low energy X-Ray Fluorescence measurements of a Glioma Associated Stem Cell. In the low left corner we report a scheme of the experiment and the sketch of the EXO-NPs. XRF maps were collected at 1 keV at the TwinMic beamline of Elettra synchrotron.[11]

Acknowledgments

References

1. Thery C., F1000 Biology Reports 2011:3;15
2. Webber J., et al. Cancer Res 2010;70: 9621
3. Cho J.A., et al. Gynecol Oncol 2011;123:379
4. Gu J., et al. PLoS One 2012; 7: e52465
5. Cho J.A., et al. Int J Oncol 2011; 40:130
6. Bourkoula E., et al. Stem Cells 2014; 32:1239
7. Malucelli E., et al. Anal Chem 2014;86:5108
8. Beltrami A.P., et al. Blood 2007;110:3428
9. Banchelli M., et al. Phys Chem Chem Phys 2014;16:10023
10. Marmorato P., et al. Toxicology Letters 2011; 207:128
11. Gianoncelli A., et al. J Synchr Rad 2016;23: 1526

Nanomechanical characterizations with contact resonance atomic force microscopy

D. Passeri,[1] M. Reggente,[1,2] M. Natali,[1] L. Angeloni,[1,3] A. Carradò,[2] M. Rossi[1,4]

[1]Department of Basic and Applied Sciences for Engineering, SAPIENZA University of Rome, Via A. Scarpa 16, 00161 Rome, Italy
[2]Institut de Physique et Chimie des Matériaux de Strasbourg (IPCMS), UMR 7504 CNRS-Université de Strasbourg, 23 rue du Loess, BP 43 67034, Strasbourg – France
[3]Lab. for Biomaterials and Bioengineering (CRC-I), Dept. Min-Met-Materials Eng. & University Hospital Research Center, Laval University, Quebec City, Canada
[4]Research Center for Nanotechnology applied to Engineering of SAPIENZA University of Rome (CNIS), Piazzale A. Moro 5, 00185 Rome, Italy

Corresponding author: Dr. D. Passeri (daniele.passeri@uniroma1.it)

Key words: contact resonance AFM, elastic modulus, viscoelasticity, nanomechanical map.

Introduction

Accurate mechanical characterization of nanomaterials and nanosystems is fundamental to achieve advancements in a broad range of applications, e.g., in nano-electromechanical systems, nanocomposites, coatings, as well as in nano-biotechnology. Materials to be characterized vary from hard protective coatings to soft polymers or biological samples. Standard methods such as nanoindentation, tensile tests, or ultrasound-based techniques, can be limited in the analysis of nanomaterials due to their poor spatial resolution and the difficulty in selecting specific locations on the sample surface and/or requiring macroscopic specimens. Also, depending on sample dimensions and mechanical properties, standard tests like nanoindentation can be destructive. Finally, results obtained with conventional methods on thin films on substrates can be dramatically affected by the mechanical properties of the substrate itself. Therefore, innovative techniques enabling truly nondestructive, accurate and reliable mechanical characterizations of nanosized volumes of materials, with nanometer scale positioning, must be developed. Atomic force microscopy (AFM) has been demonstrated to be a powerful platform for the development of methods for mechanical characterizations at the nanoscale. Among them, contact resonance AFM (CR-AFM) allows one to measure the local elastic modulus of materials by analyzing the resonances of the cantilever when the tip is in contact with the sample surface.[1] Here, we describe CR-AFM technique and give a synthetic overview of the current capabilities of this technique.

Results and Conclusions

CR-AFM is a contact mode technique in which out-of-plane oscillations at ultrasonic frequencies of the system constituted by the cantilever, the tip, and the sample are excited through a piezoelectric transducer coupled with the cantilever holder or with the sample back surface. By analyzing the resonances of the system, the contact resonance frequencies (CRFs) of the cantilever are measured, which can be used to evaluate the local indentation modulus of the sample.[2] Taking advantage of the 'stiffening' of the cantilever at ultrasonic frequencies, CR-AFM allowed the nanomechanical characterization and the indentation modulus mapping of relatively stiff samples, which cannot be studied with AFM based indentation.[3] As an example, Figure 1 shows the topography (left) of a diamond-like carbon (DLC) coating deposited with laser ablation from a glassy carbon target to a molybdenum substrate. The map of the second CRF (center) shows dark agglomerates which indicate less stiff regions. The corresponding indentation modulus map (right) allows us to evaluate the indentation modulus of the stiffer region (higher content of sp^3 carbon) in the range 160-230 GPa. The softer agglomerates, with indentation modulus of 40-50 GPa, indicate sp^2 carbon deposited on the target without bond rearrangement.[3]

Since its invention, CR-AFM has been constantly

improved to enable more accurate characterization of different mechanical parameters of broader classes of materials. For instance, by exciting shear waves in the sample and analyzing both flexural and torsional CRFs of the cantilever, Hurley and Turner used CR-AFM to independently evaluate sample Young's modulus and Poisson ratio.[4]

A major improvement of CR-AFM is represented by the possibility of characterizing viscoelastic materials, the mechanical response of which can be described by a complex elastic modulus, the real and imaginary part of which are the storage and loss modulus modulus, respectively. By acquiring the cantilever CRFs and the corresponding quality factors, indeed, storage and loss moduli as well as their ratio, i.e., the loss tangent, can be evaluated.[5] These viscoelastic parameters can be mapped with nanometer lateral resolution and, thus, CR-AFM is a powerful tool in the study of polymer blends.[6] Moreover, the sample can be mounted on a temperature controlled heating stage in order to measure and map the elastic and viscoelastic moduli of the sample at variable temperature.[7,8] Finally, the use of CR-AFM for the characterization of viscoelastic properties of soft materials at the solid-liquid interface has been reported.[9]

In conclusion, CR-AFM is a powerful technique for nanomechanical characterizations, greatly improved since its invention in terms of accuracy, range of measurable elastic moduli, accessible mechanical properties, in liquid or at variable temperature. CR-AFM is expected to be further improved, e.g., to allow the investigation of softer samples like biological materials.

References

1. Rabe U., et al. Rev Sci Instrum 1996;67:3281
2. Passeri D., et al. Rev Sci Instrum 2005;76:093904
3. Passeri D., et al. Appl Phys Lett 2006;88:121910
4. Hurley D.C., Turner J.A. J Appl Phys 2007;102:033509
5. Yuya P.A., et al. J Appl Phys 2011;109:113528
6. Yablon D.G., et al. Macromolecules 2012;45:4363
7. Natali M., et al. AIP Conf Proc 2016;1749:020007
8. Natali M., et al. AIP Conf Proc 2016;1749:020008
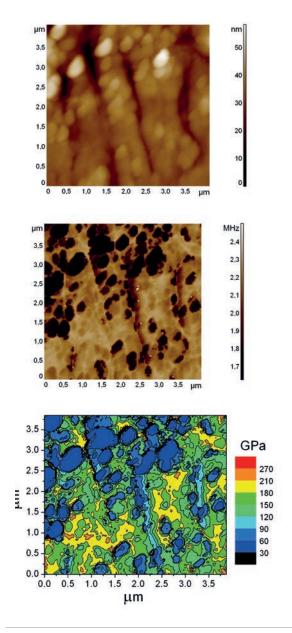9. Allison B., et al. Langmuir 2015;31:11143

Figure 1. Atomic Force Microscopy topographic image and corresponding elemental maps from low energy X-Ray Fluorescence measurements of a Glioma Associated Stem Cell. In the low left corner we report a scheme of the experiment and the sketch of the EXO-NPs. XRF maps were collected at 1 keV at the TwinMic beamline of Elettra synchrotron.[11]

Ultrasonic Force Microscopy and subsurface imaging of two-dimensional materials

P. Pingue,[1] F. Dinelli,[2] O. Kolosov[3]

[1]Laboratorio NEST - Scuola Normale Superiore, and Istituto Nanoscienze - CNR, Piazza San Silvestro 12, I-56127 Pisa, Italy
[2]CNR, Istituto Nazionale di Ottica (INO), via Moruzzi 1, 56124 Pisa, Italy
[3]Physics Department, Lancaster University, Lancaster, LA1 4YB, UK

Corresponding author: Dr. P. Pingue
(pasqualantonio.pingue@sns.it)

Introduction

Scanning probe Microscopy (SPM) represents a powerful tool that, in the past thirty years, has allowed one to investigate material surfaces in unprecedented ways at the nanoscale level. However, SPM's have shown very little power of depth penetration, whereas several nanotechnology applications would require it. Subsurface imaging has been achieved only in a few cases, when subsurface features influence the physical properties of the surface, such as the electronic states or the heat transfer. Ultrasonic Force Microscopy (UFM), an adaption of the contact mode Atomic Force Microscopy (AFM) contact mode, can dynamically measure the stiffness of the elastic contact between the probing tip and the sample surface. In particular, UFM has proven highly sensitive to the modulation of the near-surface elastic field due to the presence of non-homogeneous structures in the subsurface.

In this paper, we present an investigation of two-dimensional (2D) materials, namely flakes of graphite and molybdenum disulphide placed on structured polymeric substrates. We show that UFM can non-destructively distinguish suspended and supported areas. Specifically, UFM can probe small variations in the local indentation induced by the mechanical interaction between the tip and the sample. Therefore, any local change in the elastic modulus within the volume perturbed by the applied load or the flexural bending of the suspended areas can be detected and imaged.

Materials and Methods

Ultrasonic Force Microscopy (UFM) is a technique invented by Kolosov and Yamanaka,[1] resulting from an adaption of Atomic Force Microscopy (AFM) working in Contact Mode (CM-AFM). UFM has specifically proven a valid tool to localize subsurface defects in materials.[2] This can be achieved working at very low load values and eliminating the shear stress at contact thanks to a superlubricity phenomenon ultrasonically induced.[3]

We have carried out a study of samples made of very stiff two dimensional (2D) materials,[4] targeting the exploration of subsurface details and buried interfaces by means of UFM. In particular, we have deposited thin flakes of graphite and molybdenum disulphide (MoS$_2$) on structured polymeric substrates in order to obtain suspended and supported areas (see a schematic of the experimental setup in Figure 1A). UFM data are also compared to topographic data obtained with tapping mode AFM (TM-AFM).

Graphite or MoS$_2$ thin flakes can be transferred to a given substrate exploiting a PDMS stamp based technique.[5] In our case the substrate chosen is a film of Cyclic Olefin Copolymer (COC) polymer patterned via hot embossing in order to produce periodic flat mesas with randomly distributed voids in the regular array of grooves on a macroscopic scale (around 5x5 mm^2). The height and the periodicity of the grooves are approximately 250 nm and 1 µm, respectively. Given the typical lateral size of the flakes in the range from 5 to 20 µm, they present adjacent regions alternatively supported by the COC mesas and suspended over the voids (see Figure 1 B).
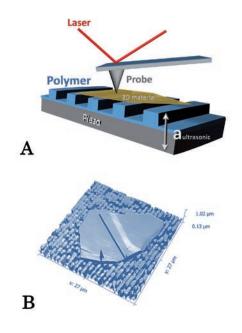

Figure 1. (A) Schematic of the experimental setup. (B) Topographic image of a graphitic flake on top of a patterned COC substrate.

The UFM setup is based on a standard CM-AFM including a vibrating sample stage, capable of producing out-of-plane ultrasonic vibrations with amplitude $a_{ultrasonic}$. These vibrations are transferred to the specimen, reversibly bonded to the stage, while the AFM tip and the sample surface are in contact under a fixed average load F_N. Our experimental setups are hybrid systems made of commercial and custom components, that can perform both UFM and TM-AFM measurements. One is based on a *Multimode*-type head with a *Nanoscope III* controller (Bruker), the other on a *SMENA*-type head (NT-MDT) with home-built electronic controller. Both these systems are equipped with a custom sample holder made of a piezo disc with having a thickness typical resonance around 2 or 4 MHz (Physik Instrumente).
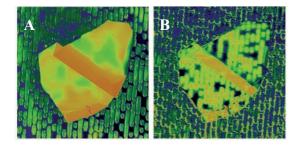
Results and Conclusions

In Figure 2 A-B, we show some data obtained for a graphite flake (around 50 nm in thickness, excluding folded areas) deposited on a patterned COC film, as described above. Figure 2 A shows the topography obtained with standard TM-AFM: the topography image is featureless and smooth, and it is not possible to identify suspended or supported regions within the flake.

Figures 2 B shows the same flake imaged with UFM: the nanomechanical UFM contrast clearly discriminates the supported from the suspended portions of the flake, the latter appearing darker. Finally, in Figure 2 C the superposition of a UFM image with a topography one (also obtained with standard TM-AFM) of a MoS$_2$ flake is presented: again the presence of voids underneath the flake is well visible (darker contrast).

In summary, we have shown how UFM can detect and image subsurface features on the nanoscale in the case of two-dimensional materials, namely graphite and molybdenum disulphide.[6] In particular, we have investigated flakes of a few tens of nanometres in thickness placed on structured polymeric substrates with suspended and supported areas. We have demonstrated that UFM can identify the different regions in a non-destructive way, as is it highly sensitive to the flexural bending induced by the elastic field applied by the tip on the sample.

For all these reasons, we believe that this particular SPM technique is a very promising candidate for the mechanical characterization and testing of nano-devices based on 2D-materials where high spatial resolution may be requested.
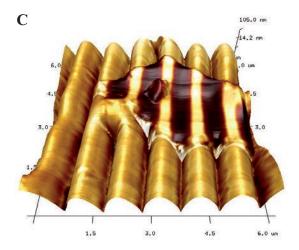

Figure 2. (A) Topography image of a graphitic flake on deposited on top of the patterned COC substrate. **(B)** UFM image of the same graphene flake showing a contrast due to its subsurface imaging capability. **(C)** UFM image superimposed to a topographic one of a MoS$_2$ flake: also in this case UFM demonstrates its subsurface sensitivity showing the presence of grooves under the 2D-material flake. The topography images were both obtained with TM-AFM.

References

1. Kolosov O.V., Yamanaka K. J Appl Phys Part 2-Letters 1993;32:L1095
2. Dinelli F., et al. Appl Phys Lett 1997;71:1177
3. Yamanaka K., et al. Appl. Phys. Lett 1994;64:178
4. Checanov A.S., et al. IEEE Trans Magn 1996;32:3696
5. Dinelli F., et al. Phil Mag A 2000:80:2299
6. Novoselov K.S., et al. Proc Nat Acad Sci 2005;102:10451
7. Goler S., et al. J Appl Phys 2011;110:064308.
8. Dinelli F., et al. Nanotechnology (in publication)